Eur. Phys. J. A **16**, 43–50 (2003)
DOI 10.1140/epja/i2002-10072-2

THE EUROPEAN PHYSICAL JOURNAL A

Pre- and post-scission neutron multiplicities in $^{19}F + ^{209}Bi$ reaction at 108 MeV

L.M. Pant[1,a], A. Saxena[1], R.G. Thomas[1], D.C. Biswas[1], and R.K. Choudhury[2]

[1] Nuclear Physics Division, Bhabha Atomic Research Centre, Mumbai 400085, India
[2] Institute of Physics, Bhubaneshwar, India

Received: 15 March 2002 / Revised version: 23 August 2002 /
Published online: 17 January 2003 –
Communicated by W. Henning

Abstract. The pre- and post-scission neutron multiplicities have been determined from the fragment-neutron angular-correlation measurements in $^{19}F + ^{209}Bi$ reaction at bombarding energy of 108 MeV. The average pre-scission neutron multiplicity (ν^{pre}) is significantly larger than that calculated on the basis of the statistical model. The excess in ν^{pre} value is used to estimate the dynamical delay in the fusion-fission time scale for the ^{228}U compound system. For a level density parameter $a_n = A/10$ MeV^{-1} and $a_n = a_f$, the fusion-fission dynamical time was established to be $120 \pm 10 \times 10^{-21}$ s. We also observe that ν^{pre} is higher for asymmetric mass splits as compared to symmetric mass splits. The enhancement in the ν^{pre} for the asymmetric region could be due to strong variations in the fragment mass distribution at different stages in multiple chance fission at medium excitation energies.

PACS. 25.70.Jj Fusion and fusion-fission reactions

1 Introduction

Measurements of pre-scission neutron multiplicities in heavy-ion–induced fusion-fission reactions provide useful information on fission dynamics and the effects of nuclear viscosity on the fission process [1–3]. There have been a lot of measurements over the last decade on the pre-scission particle multiplicities for a large number of systems. Hinde *et al.* [4] measured the fragment-neutron angular correlations for the compound nuclei ^{168}Yb, $^{192,198,200}Pb$, ^{210}Po, ^{213}Fr and ^{251}Es formed at excitation energies between 45–90 MeV. They observed that the statistical model code underestimates the pre-scission particle multiplicities and the discrepancy increases with excitation energy and fissility. It is generally observed in many heavy- and light-ion–induced reactions that the measured pre-scission neutron multiplicities are much higher than that expected on the basis of statistical model calculations. The excess neutron emission from the composite fissioning system has been interpreted to be due to a time delay in the fission process arising due to dynamical effects in the fission decay. It has been found that the fusion-fission time scales depend on fissility, entrance channel mass asymmetry of the interacting nuclei and the ratio of fission barrier to temperature, (B_{fis}/T) of the fissioning nucleus [3]. From the systematic measurements, it is also observed that the Businaro-Gallone critical mass asymmetry plays an important role in deciding the delay in the formation stage of the compound nucleus in the fusion-fission process. The time scales of nuclear fission have been extensively studied [4,5] up to nuclear temperatures of about 2.7 MeV. Hilscher *et al.* [6] deduced time scales of fission at nuclear temperatures of 5 MeV for $^{32}S + ^{144,154}Sm$. They also observed that the pre-scission lifetime for fission with symmetric mass splits is longer than for asymmetric mass splits. Symmetric mass splits can be associated with fission from a fully equilibrated system in energy and mass degree of freedom resulting probably from more central collisions than asymmetric mass splits which carry more angular momentum and may have contributions from fast-fission events. The dependence of ν^{pre} on the fission fragment mass and on the total kinetic energy was measured for the reaction of 215 MeV ^{20}Ne on ^{232}Th by Hinde *et al.* [7]. No variation was found except for the lowest values of the TKE, where a reduction in multiplicity was observed. In a separate measurement Hinde *et al.* [8] also measured pre-scission and post-scission neutron yields as a function of projectile mass, compound nucleus fissility, fission mass ratio and total kinetic energy (TKE) for a large number of fusion-fission reactions induced by $^{16,18}O$, ^{40}Ar and ^{64}Ni beams on different targets ($^{nat}UF_4$, ^{197}Au, ^{169}Tm, ^{154}Sm, ^{144}Sm, ^{208}Pb, ^{165}Ho, ^{141}Pr and ^{184}W). All these results showed that ν^{pre} falls quite rapidly with in-

[a] e-mail: lalit_pant@rediffmail.com; lalit.pant@exp2.physik.uni-giessen.de

creasing mass asymmetry and have been attributed to a reduction of the dynamical fission time scale with mass asymmetry. Some of these reactions also have appreciable fraction of quasi-fission and fast-fission events. They also observed that there was no dependence of $\nu^{\rm pre}$ on TKE.

A new model of nuclear scission (the random neck rupture model [9]) has been developed, which gives unique predictions of the variation of the post-scission neutron multiplicity $\nu^{\rm post}$ with mass split. This model naturally leads to the experimentally observed widths of mass distributions and predicts the sawtooth behaviour in $\nu^{\rm post}(A)$ at low excitation energies [10]. Experimental data both in support of and in conflict [11,12] with the resulting energy sharing as a function of mass split have been published. The validity of Brosa's model has been effectively investigated by Hinde *et al.* [12] comparing the predictions with measurements for a system near ^{252}Cf (for which extensive spontaneous-fission measurements have been made) produced at high excitation energy in a heavy-ion fusion reaction. They measured the variation of $\nu^{\rm pre}$ and $\nu^{\rm post}$ with mass split for the fission of ^{19}F + ^{232}Th at bombarding energies of 105 and 120 MeV and observed that the post-scission multiplicities show no evidence for the persistence of the sawtooth yield observed for the spontaneous fission of ^{252}Cf. Recently Samant *et al.* [13] observed fission fragment anisotropies in ^{19}F + ^{209}Bi system in agreement with the saddle point statistical model calculations over a range of bombarding energies, thereby concluding that the spherical target plus projectile system behave normal from near to above barrier energies. This observation is in contrast to the findings of Hinde *et al.* [14] where they measured fusion cross-sections for ^{19}F + ^{208}Pb, which is also a spherical system and have reported that statistical model calculations of the fission anisotropies were unable to reproduce the observed dependence on beam energy. It has also been recently observed by Pant *et al.* [15] that in the case of the ^{19}F + ^{209}Bi system there is some noticeable enhancement in the variation of the total kinetic energy near the barrier region. In view of the above exciting results, we were motivated to explore the dynamics of fusion-fission in ^{19}F + ^{209}Bi system as a function of neutron multiplicity. In the present work, we discuss our results on the measurements of neutron multiplicities in the fission of the ^{19}F + ^{209}Bi system at 108 MeV of bombarding energy. The neutron multiplicity has also been measured as a function of symmetric and asymmetric mass splits. Section 2 gives the details of the experimental set-up. Section 3 deals with the data analysis procedure. Section 4 contains the results of the present work. The summary and conclusions are given in sect. 5.

2 Experimental set-up

The experiments were carried out at the 14MV BARC-TIFR Pelletron Accelerator Facility at Mumbai. We have studied the mass dependence of neutron multiplicity by measuring the fragment-neutron angular correlations along and perpendicular to the fission direction for the ^{19}F + ^{209}Bi system at 108 MeV of projectile energy. The

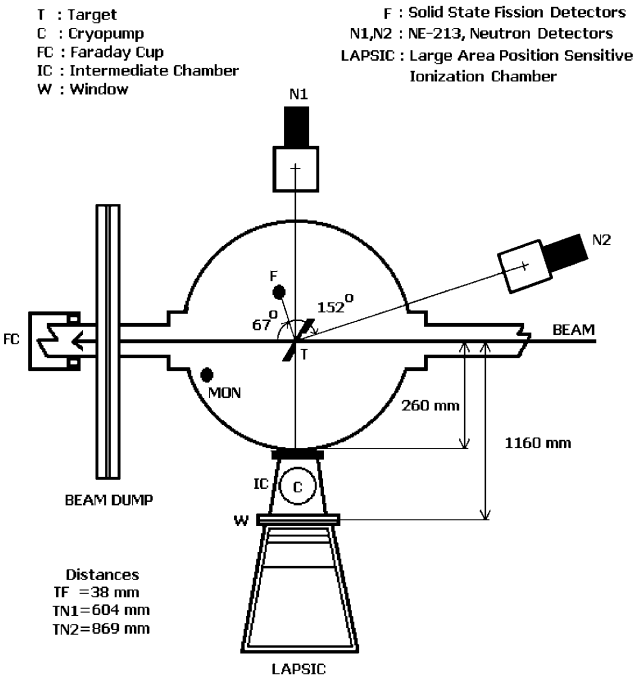

Fig. 1. Schematic diagram of the scattering chamber along with the orientation of a silicon surface barrier detector telescope (F), NE-213 liquid-scintillator neutron detectors (N1, N2) and the LAPSIC with respect to the beam.

^{209}Bi target used in the measurement had a thickness of $600\,\mu$g/cm^2. The schematic diagram of the experimental set-up is shown in fig. 1. In this arrangement a silicon surface barrier detector telescope (F) was kept at 67° with respect to the beam direction for detection of fission fragments. The silicon detector telescope consisted of a transmission-type surface barrier detector, ΔE of 25 μm thickness backed with a 1 mm thick E detector. In the telescope, the E detector were operated in anticoincidence mode with respect to the ΔE detector to filter out any possible contamination of beam-like particles with the fission events in the ΔE detector. It was further collimated to subtend an angular coverage of $\pm\,4.5°$ at the target center. The LAPSIC [15,16], kept at the mean angle of 90° with respect to the beam, subtended an angle of $\pm\,11°$ in the reaction plane. The angular openings of the surface barrier detector telescope and the LAPSIC in the reaction plane were such that the fission folding angle distribution for the full momentum transfer in ^{19}F + ^{209}Bi reaction at 108 MeV bombarding energy were well covered by the detector configuration. The ΔE and E signals from the LAPSIC and similar energy signals from the silicon surface barrier detector telescope were recorded event by event for further off-line analysis. The neutrons were detected by two $6''\phi \times 5''$ thick NE-213 neutron detectors. One of the NE-213 neutron detectors was kept at 90° (N1), and the other at 152° (N2), to catch the neutrons along and perpendicular to the fission direction. The mass dependence of the neutron multiplicities was determined by measuring the neutrons emitted in coincidence with the pair of fission fragments detected in the surface barrier

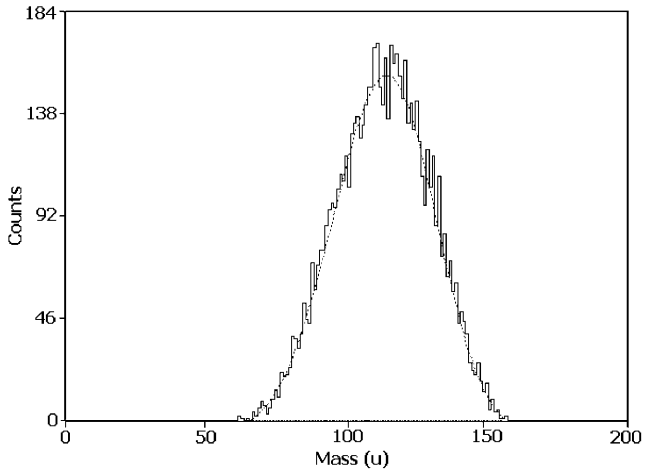

Fig. 2. A typical mass distribution spectrum for $^{19}F + ^{209}Bi$ reaction at $E_{lab} = 108$ MeV, along with the fit.

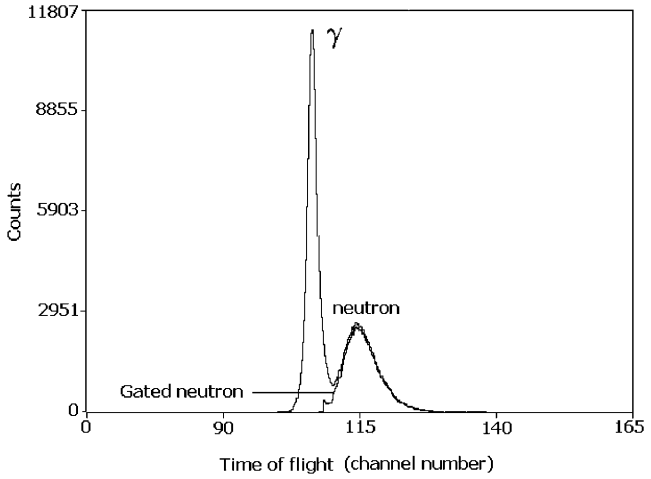

Fig. 3. Time-of-flight spectra for neutrons and gammas as observed in an NE-213 liquid-scintillation neutron detector with and without the neutron gate for the $^{19}F + ^{209}Bi$ reaction at $E_{lab} = 108$ MeV.

detector telescope and LAPSIC, which was operated at a pressure of 14 mbar with P-10 gas in flow mode. The beam dump was situated 2.5 meters away from the target center and the beam dump shield consisted of a layer each of borated paraffin and lead bricks to shield the NE-213 neutron detectors from intense neutron and gamma-ray background generated by the beam falling on the Faraday Cup. The distances of the neutron detectors N1 and N2 from the target center were 604 mm and 869 mm, respectively. The pulse shape discrimination property of the NE-213 detectors was used to differentiate neutrons from the gamma-rays. To detect the coincident binary fragments a time correlation was established by taking the start signal from the LAPSIC and the stop signal from the F detector using a time-to-amplitude converter. The energy calibration of the detectors for fission fragments was done using a ^{252}Cf spontaneous-fission source. The pulse heights from the two detectors were converted into the post-scission kinetic energies of the two fragments by an event-by-event iterative analysis. The pulse height defect in the surface barrier detector were corrected by the mass-dependent energy calibration procedure using the parameters given by Wiessenberger *et al.* [17]. The energies of the fission fragments were determined by incorporating in the data analysis the corrections due to energy loss in the target foil, polypropylene window and the gas dead layer at the entrance of the ionization chamber. The total average energy loss for the most probable fragments in the ^{209}Bi target, the polypropylene window and the gas dead layer of the chamber was seen to be in the range of 15–21 MeV, which could be corrected in the present analysis. The center-of-mass energies of the fragments were derived after kinematic transformation assuming full momentum transfer to the compound nucleus. These energies were further corrected for neutron evaporation effects to obtain the pre-neutron emission masses by using the mass and momentum conservation relations. For neutron evaporation corrections, we have taken the available data on the systematics for the post-scission neutron multiplicities as a function of fissility [3,18] and assuming neutron evaporation to be proportional to the fragment mass. These corrections were of the order of 1.5 to 2.0 MeV. The kinetic energy and mass distributions of the fission fragments as measured by the two detectors were found to agree well with each other, implying that the correction factors in both the detectors have been taken into account in a consistent manner. Figure 2 shows the mass distribution spectrum along with the fit, obtained for the $^{19}F + ^{209}Bi$ system at 108 MeV bombarding energy with the peak position at 114 u and a FWHM of 42 u. The neutron detection efficiency was determined by Monte Carlo simulations.

3 Data analysis

The neutron energy was measured by the time of flight of neutrons with respect to the fission fragments. The neutron energy spectra were determined from the observed time-of-flight spectra after correcting for the neutron detection efficiency for each neutron detector. The master gate was generated by taking a twofold coincidence between a) time of flight from N1 (FN1), b) time of flight from N2 (FN2) and c) the prescaled fission singles. For the mass dependence of neutron multiplicities the TAC generated by the two complementary fragments detected, respectively, in F and LAPSIC were also recorded whenever fission neutron coincidence was present. The position of the gamma peak was used as reference for calibrating the neutron time-of-flight spectra. The spread in the time-of-flight signal with respect to the fragment pulse height was corrected in the off-line analysis. The time resolution, as determined from the FWHM of the gamma peak, was found to be 2.5 nanoseconds. Gates were put along the neutron region in the 2D plots of pulse shape discrimination *versus* pulse height as well as that along the time of flight *versus* pulse shape discrimination. The above gates are used to extract neutrons in coincidence

with the fission events and are shown in fig. 3 in the time-of-flight spectrum for ^{19}F + ^{209}Bi reaction at 108 MeV bombarding energy. The coincidence data were analysed event by event to obtain the information on the fragment mass and the neutron energy. The results were obtained for the combinations of fragment-neutron detectors along and perpendicular to the fragment emission direction. The fragment mass dependence of the neutron energy was obtained by placing broad gates on the fragment mass in the 2D plots of the neutron energy *versus* fragment mass generated from the experimental data. The neutron energy spectra thus obtained were analyzed to obtain the pre-scission and post-scission components by the moving source fit procedure given below.

Moving source fit analysis

The parameters for pre-scission and post-scission components are derived by carrying out moving source fits to the observed neutron energy spectra. It is assumed that pre-scission neutrons are emitted from a source moving with the center-of-mass velocity of the compound system. The emission of the post-scission neutrons is from the two fully accelerated fragments. In both cases, emission from the rest frame of the emitting system is assumed to be isotropic. Within this assumption the cross-section of neutrons evaporated from all the three sources is given by the Watt expression [19]

$$\frac{\mathrm{d}^2\sigma}{\mathrm{d}E_\mathrm{n}\mathrm{d}\Omega_\mathrm{n}} = \sum_{i=1}^{3} \frac{\nu_i^\mathrm{n}\sqrt{E_\mathrm{n}}}{2(\pi T_i)^{3/2}} \times \exp\left(\frac{-(E_\mathrm{n} - 2\sqrt{\epsilon_i E_\mathrm{n}}\cos\phi_i + \epsilon_i)}{T_i}\right), \quad (1)$$

where ϵ_i, T_i and ν_i^n are the energy per nucleon, temperature and the multiplicity of each neutron source, i, respectively. E_n is the laboratory energy of the neutron and ϕ_i is the neutron detection angle with respect to the source, i. The value of ϵ_i for the composite nucleus was calculated assuming full momentum transfer to the compound nucleus, as the contribution due to transfer-induced fission is expected to be small for the ^{19}F + ^{209}Bi system at the bombarding energy used in the experiment. The ϵ_i values for the two fission fragments and the angle of the emission of the complementary fragment were determined using Viola's systematics for the total kinetic energy release in symmetric fission [20] which is given below

$$\mathrm{TKE} = (0.107)\frac{Z^2}{A^{\frac{1}{3}}} + 22.2\,\mathrm{MeV}\,, \quad (2)$$

Z and A are atomic number and atomic mass of the compound nucleus. The laboratory energies of the two fission fragments and the laboratory angle of the complementary fragment were calculated using reaction kinematics corresponding to symmetric mass division after taking into account the recoil of the composite nucleus. The post-scission parameters ν^post and T^post were assumed to be equal for both the fragments in case of symmetric fission. In case of asymmetric mass splits, the mean fission fragment velocities were calculated using a different expression [20] for the total kinetic energy, which is dependent on the charge and mass of the two fission fragments, Z_1, Z_2, A_1 and A_2 and given as

$$\mathrm{TKE} = (0.755)\frac{Z_1 Z_2}{\left(A_1^{\frac{1}{3}} + A_2^{\frac{1}{3}}\right)} + 7.3\,\mathrm{MeV}\,. \quad (3)$$

The post-scission parameter, ν^post was taken to be proportional to the ratio of the fragment masses for asymmetric splits. The four parameters, ν^pre, T^pre, ν^post and T^post were obtained by fitting the observed neutron energy spectra with the expression in eq. (1) by chi-square minimization procedure.

4 Results and discussion

Singles measurements

In the first set of measurements, neutrons in N1 (90°) and N2 (152°) were detected in coincidence with the fission singles in the F detector. The results of these measured neutron energy spectra from the possible geometrical combinations of the fission detector (F) and the neutron detectors (N1,N2) are shown in fig. 4. These spectra correspond to fragment-neutron correlations of FN1 ($\theta_\mathrm{nf} \sim 23°$), and FN2 ($\theta_\mathrm{nf} \sim 85°$). As seen from fig. 4a the neutron energy spectra is less steep in case of $\theta_\mathrm{nf} \sim 23°$ because of the neutrons emitted from fully accelerated fragments, whereas for $\theta_\mathrm{nf} \sim 85°$ (fig. 4b) the neutron spectra fall somewhat more rapidly because of the larger admixture of the pre-scission events. These experimentally observed neutron energy spectra are shown along with the moving source fits for the pre-scission and post-scission components at $\theta_\mathrm{nf} \sim 23°$ and $\sim 85°$. The fits give $\nu^\mathrm{pre} = 3.11(\pm 0.30)$ and $\nu^\mathrm{post} = 0.92\ (\pm 0.12)$ with $T^\mathrm{pre} = 0.90\,\mathrm{MeV}$ and $T^\mathrm{post} = 0.63\,\mathrm{MeV}$. From the fitted values of ν^pre and ν^post the total neutron multiplicity was derived as

$$\nu^\mathrm{total} = \nu^\mathrm{pre} + 2\ \times\ \nu^\mathrm{post}\,, \quad (4)$$

which is found to be 4.95 for the present system. Hinde [7] has measured neutron multiplicities for the ^{20}Ne + ^{209}Bi reaction. This happens to be close to our system and obtained a $\nu^\mathrm{total} = 8.17 \pm 0.30$ for a compound nucleus with excitation energy equal to 76 MeV. Figure 5 shows the variation of ν^total with excitation energy of the compound nucleus taken from ref. [3] for different target-projectile combinations along with the findings of the present work. This figure shows that the present data is consistent with the increase in total neutron multiplicity as a function of excitation energy of the compound nucleus observed earlier for different fissioning systems. Figure 6 shows the value of ν^pre (filled circle) measured in this work alongwith the results of ALICE (dashed line) and PACE2 (dotted line) calculations using a level density parameter equal

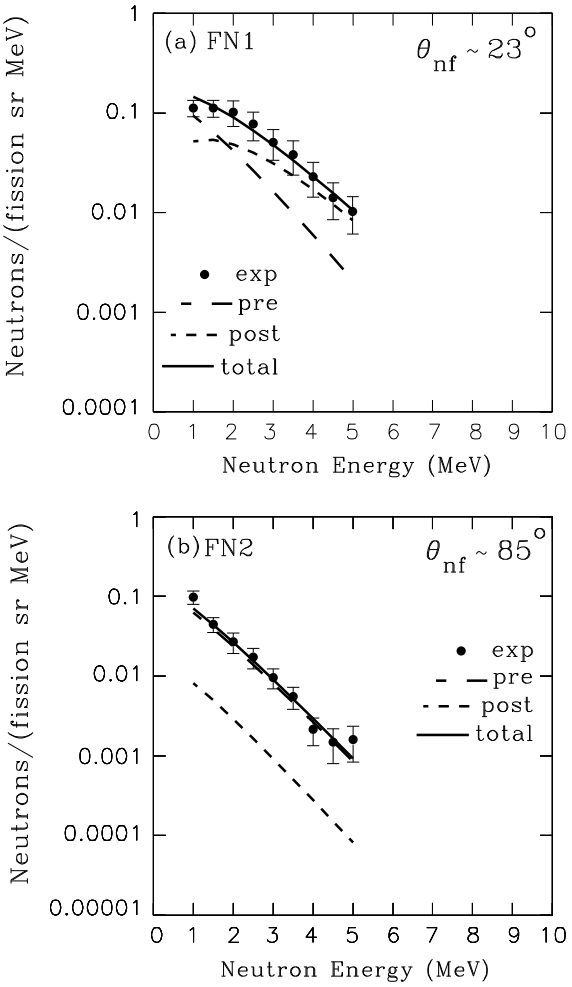

Fig. 4. The experimentally observed neutron energy spectra along with the fits for the pre-scission and post-scission components for the ^{228}U compound system, (a) $\theta_{nf} \sim 23^{\circ}$. (b) $\theta_{nf} \sim 85^{\circ}$.

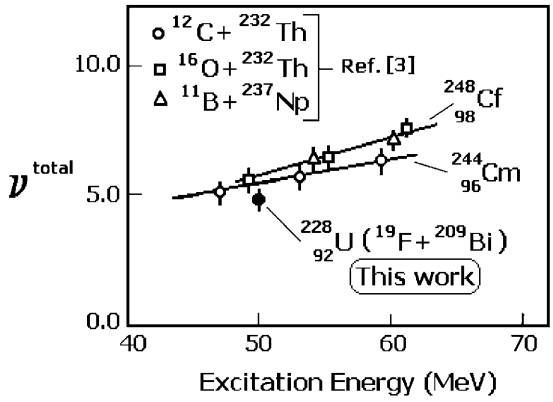

Fig. 5. Total neutron multiplicities, $\nu^{\rm total}$, plotted as a function of excitation energy and fissility of the compound nucleus for different systems (ref. [3]), along with the present work.

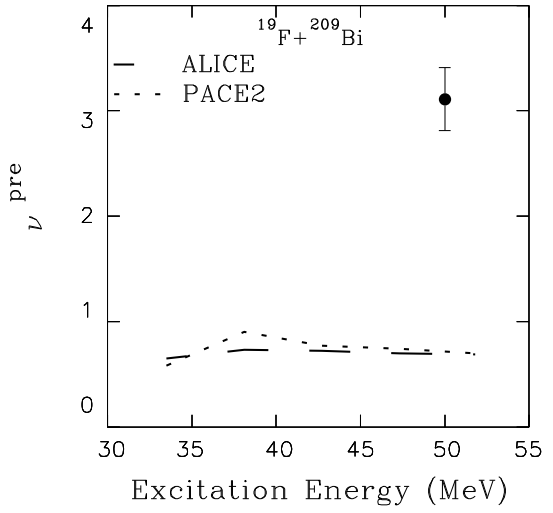

Fig. 6. The experimental value of $\nu^{\rm pre}$ (filled circle), measured in this work, as a function of the excitation energy of the ^{228}U compound system at 108 MeV bombarding energy. The results of ALICE (dashed line) and PACE2 (dotted line) calculations using a level density parameter equal to $A_{\rm cn}/10\,{\rm MeV}^{-1}$ are also shown in the figure.

to $A_{\rm cn}/10\,{\rm MeV}^{-1}$, as a function of the excitation energy of the ^{19}F + ^{209}Bi compound system. It is seen from fig. 6 that the measured values are much higher than the statistical model calculations. Therefore, considerable number of neutrons are emitted in the fission process over and above those expected from the statistical phase space considerations. This result implies that there is large amount of time delay involved in the fission process in this reaction. The excess number of pre-scission neutrons, $\nu^{\rm pre}$(excess) can be related to the total dynamical time available in the fusion-fission process and is expressed as

$$\nu^{\rm pre}({\rm excess}) = \nu^{\rm pre}({\rm measured}) - \nu^{\rm pre}({\rm calculated})\,, \quad (5)$$

where $\nu^{\rm pre}$(calculated) is the value predicted by the statistical model. By using the relation

$$\tau_{\rm fission} = \sum_{i=1}^{\nu^{\rm pre}({\rm excess})} \frac{\hbar}{\Gamma_{\rm n}(E^*)} \quad (6)$$

the dynamical fission times $\tau_{\rm fission}$ of the fissioning system can be deduced from the number of excess neutrons, $\nu^{\rm pre}$(excess). Thus a given $\nu^{\rm pre}$ can be mapped directly to the time since formation of the nucleus. The $\tau_{\rm fission}$ value as deduced from this analysis is found to be 120 ± 10 × 10^{-21} s for the ^{19}F + ^{209}Bi system, corresponding to a level density parameter $a_{\rm n} = A/10\,{\rm MeV}^{-1}$ and $a_{\rm n} = a_{\rm f}$.

M1-M2 dependence of neutron multiplicities

In our second set of measurements we have put the further constraint of demanding the coincidence between the two fragments (M1-M2) which are thus detected in coincidence in the surface barrier detector and the LAPSIC. To look for the effect of different mass splits on the neutron multiplicity, we selected a broad mass regions for this purpose. For the symmetric case, the mass window was selected from 104 u to 124 u, *i.e.* ± 10 mass units

Table 1. Mass split dependence of neutron multiplicities for ^{19}F + ^{209}Bi system at $E_{\rm lab} = 108$ MeV.

Neutrons in coincidence with	$\nu^{\rm pre}$	$2\times(\nu^{\rm post})$	$\nu^{\rm total}$	$T^{\rm pre}$ (MeV)	$T^{\rm post}$ (MeV)
fission singles in F only	3.11 ± 0.30	1.84 ± 0.12	4.95 ± 0.32	0.90	0.63
M1-M2 dependence (symmetric region) (104 u to 124 u)	2.83 ± 0.25	1.58 ± 0.11	4.41 ± 0.27	1.00	0.56
M1-M2 dependence (asymmetric region) (125 u to 145 u)	3.31 ± 0.31	2.24 ± 0.15	5.55 ± 0.34	0.58	1.35

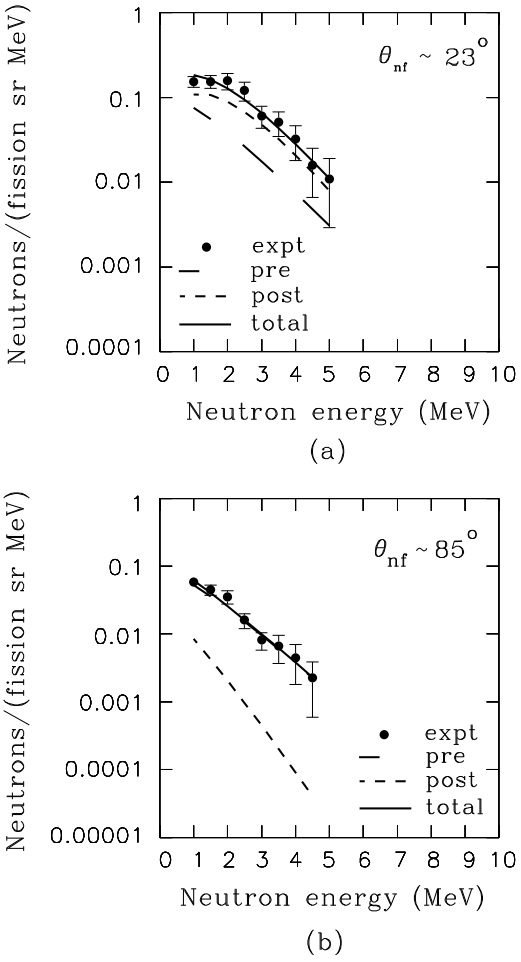

Fig. 7. Neutron energy spectra along with the fits for the pre-scission and post-scission components are shown for (a) $\theta_{\rm nf} \sim 23^\circ$ and (b) $\sim 85^\circ$ for the ^{19}F + ^{209}Bi system for a symmetric mass window (104 u to 124 u).

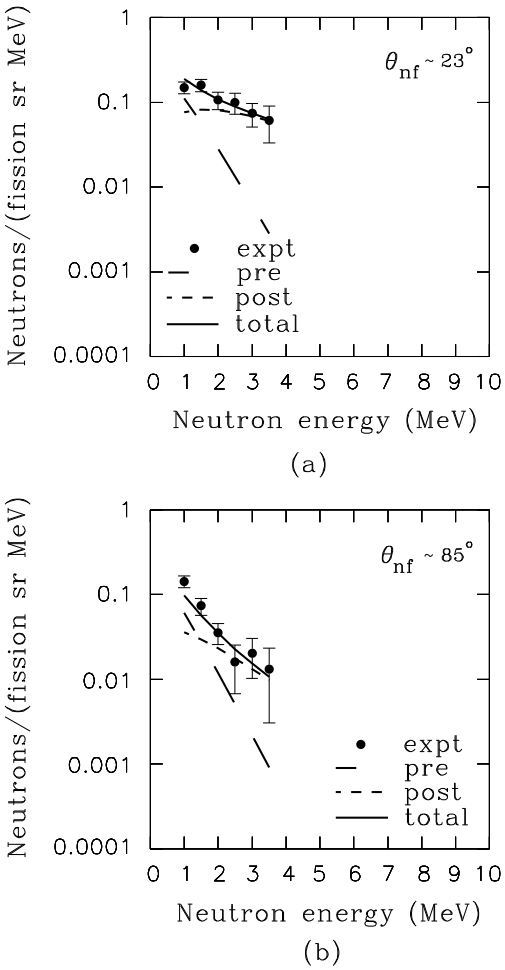

Fig. 8. Neutron energy spectra along with the fits for the pre-scission and post-scission components are shown for (a) $\theta_{\rm nf} \sim 23^\circ$ and (b) $\sim 85^\circ$ for the ^{19}F + ^{209}Bi system for an asymmetric mass window (125 u to 145 u).

with respect to the symmetric mass split at 114 u, for the ^{19}F + ^{209}Bi compound system and for the asymmetric region the mass window covered 125 u to 145 u. Figures 7 and 8 show the neutron energy spectra along with the fits for the pre-scission and post-scission components for the ^{19}F + ^{209}Bi system for the symmetric and asymmetric mass splits, respectively. The values for $\nu^{\rm pre}$, $\nu^{\rm post}$, $T^{\rm pre}$ and $T^{\rm post}$ are listed in table 1 for both singles and different mass split regions. For the symmetric case the value of $\nu^{\rm pre}$ obtained was 2.83 ($\pm$0.25) which is lower than the value of $\nu^{\rm pre}$ obtained from the singles measurements (3.11$\pm$0.30). However, for the asymmetric case the value of

ν^{pre} is seen to be 3.31 (± 0.31), significantly higher than the value of ν^{pre} obtained for either symmetric split or the singles measurements. This enhanced value of ν^{pre} for the asymmetric split gives rise to an increased value of ν^{total} (5.55 ± 0.38). The value of ν^{post} also shows an enhancement for asymmetric splits. Assuming equal weight factors for symmetric and asymmetric mass windows and averaging ν^{pre} and ν^{total} from the two mass regions, we obtain $\nu^{pre}_{avg} = 3.07$ and $\nu^{total}_{avg} = 4.98$, which are similar to $\nu^{pre}_{sin}(3.11)$ and $\nu^{total}_{sin}(4.95)$, obtained in singles measurements. The enhancement in the value of ν^{pre} for the asymmetric mass region may be due to the presence of a higher-chance fission for the ^{228}U compound system. The increased value for ν^{pre} for asymmetric mass splits as compared to symmetric mass splits could be an artifact of the existence of higher-chance fission. This is because we are biasing our analysis by selecting the asymmetric mass region, which could be dominated by the multiple fission at low excitation energies. Also, the decay energy available with the fragments for the asymmetric region is about 4 MeV more as compared to the symmetric region, which could also lead to an increase in the observed values of ν^{pre}. Itkis [21] also observed in the ^{226}Th ($^{18}O + ^{208}Pb$) system, a higher value for ν^{pre} for asymmetric splits as compared to symmetric splits at a compound-nucleus excitation energy of 26 MeV and the phenomenon was attributed to the existence of channels in the evolution of a fissioning system from the ground state of a compound nucleus to the scission point. In a similar way, Strecker *et al.* [22] studied the post-scission multiplicity dependence on fragment masses for $p + ^{235,238}U$. Their data exhibits a pronounced sawtooth structure well known from spontaneous and slow-neutron–induced fission, which is attributed to the fact that ^{236}Np and ^{239}Np undergo to a considerable fraction of higher-chance fission. In contrast, Bishop *et al.* [23] observed a less pronounced sawtooth for $p + ^{233}U$ which is because of domination of first-chance fission in the ^{234}Np compound system. As the fragments of $p + ^{233}U$ reaction are equipped with more excitation energy and, therefore, show a less pronounced sawtooth. Thus, due to the presence of multiple-chance fissions, it is difficult to extract fission delay from the measurements of neutron multiplicity as a function of fragment mass. However, at higher excitation energies, first-chance fission may start dominating and probably fission delay can be extracted from neutron multiplicity measurements. These results are however not conclusive and one has to be careful as regards the existence of multiple-chance fission, at low excitation energies, in deriving any dynamical time from the observed pre-scission neutron multiplicity.

5 Conclusions

In the present work we have measured the neutron multiplicity and also looked for its M1-M2 dependence for the $^{19}F + ^{209}Bi$ reaction at a bombarding energy of 108 MeV. The measurements of neutron multiplicity show a large time delay involved in the fission process in this reaction. The ν^{pre}(excess) observed for the $^{19}F + ^{209}Bi$ reaction has been used to derive the dynamical fusion-fission time for the ^{228}U compound system. For a level density parameter $a_n = A/10\,MeV^{-1}$ and $a_n = a_f$, the fusion-fission dynamical time has been measured as $120 \pm 10 \times 10^{-21}$ s. We also observe that, from the M1-M2 dependence measurement, the ν^{pre}-value for asymmetric splits is enhanced as compared to the symmetric splits and this is attributed to variations in the fragment mass distribution at different stages in multiple-chance fission at medium excitation energies. For the mass dependent measurement we observe that ν^{pre} is enhanced for asymmetric mass splits as compared to symmetric mass splits. The enhanced ν^{pre} for the asymmetric region could be because of the presence of multiple-chance fissions. Further, by gating on asymmetric masses, one is selecting the events coming from a cooled-fissioning system resulting from the emission of a larger number of neutrons. With the possible effects due to multichance fission, it is difficult to extract fission delay as a function of fragment mass from the measurements of mass-dependent neutron multiplicities. Further studies with different target-projectile combinations at higher excitation energies will lead to a better understanding of the role of mass asymmetry in the dynamical processes involved in the heavy-ion–induced fusion-fission reactions.

We are thankful to Dr. S.S. Kapoor for many useful discussions. We are also grateful to Dr. H.C. Jain for providing us NE-213 neutron detectors. We also acknowledge the help of B.V. Dinesh, B.K. Nayak, V.P. Singh and A.L. Inkar during the course of the experiment. The help from the Pelletron accelerator staff for smooth running of the accelerator and providing necessary beams is gratefully acknowledged.

References

1. J.O. Newton, Pramana **33**, 175 (1989).
2. A. Saxena, S. Kailas, A. Karnik, S.S. Kapoor, Phys. Rev. C **47**, 403 (1993).
3. A. Saxena, A. Chatterjee, R.K. Choudhury, S.S. Kapoor, D.M. Nadkarni, Phys. Rev. C **49**, 932 (1994).
4. D.J. Hinde, R.J. Charity, G. S. Foote, J. R. Leigh, J. O. Newton, S. Ogaza, A. Chatterjee, Nucl. Phys. A **452**, 550 (19812).
5. W.P.Zank, D. Hilscher, G. Ingold, U. Jahnke, M. Lehmann, H. Rossner, Phys. Rev. C **33**, 519 (1986).
6. D. Hilscher, H. Rossner, B. Cramer, B. Gebauer, U. Jahnke, M. Lehmann, E. Schwinn, M. Wilpert, Th. Wilpert, H. Frobeen, E. Mordhorst, W. Scobel, Phys. Rev. Lett. **62**, 1099 (1989).
7. D.J. Hinde, H. Ogata, M. Tanaka, T. Shimoda, N. Takahashi, A. Shinohara, S. Wakamatsu, K. Katori, H. Okamura, Phys. Rev. C **39**, 2268 (1989).
8. D.J. Hinde, D. Hilscher, H. Rossner, B. Gebauer, M. Lehmann, M. Wilpert, Phys. Rev. C **45**, 1229 (1992).
9. U. Brosa, S. Grossmann, Z. Phys. A **310**, 177 (1983).
10. S. Grossmann, U. Brosa, Z. Phys. A **319**, 327 (1984).
11. D.R. Benton, H. Breuer, F. Khazaie, K. Kwiatkowski, V.E. Viola, S. Bradley, A.C. Mignerey, A.P. Weston-Dawkes, Phys. Rev. C **38**, 1207 (1988).

12. D.J. Hinde, J. R. Leigh, J.J.M. Bokhorst, J.O. Newton, R.L. Walsh, J.W. Boldeman, Nucl. Phys. A **472**, 318 (1987).
13. A.M. Samant, S. Kailas, A. Chatterjee, A. Shrivastava, A. Navin, P. Singh, Eur. Phys. J. A **7**, 59 (2000).
14. D.J. Hinde, A.C. Berriman, M. Dasgupta, J.R. Leigh, J.C. Mein, C.R. Morton, J.O. Newton, Phys. Rev. C **60**, 054602 (1999).
15. L.M. Pant, R.K. Choudhury, A. Saxena, D.C. Biswas, Eur. Phys. J. A **11**, 47 (2001).
16. R.K. Choudhury, D.M. Nadkarni, V.S. Ambekar, B.V. Dinesh, A. Saxena, M.S. Samant, D.C. Biswas, L.M. Pant, Pramana **44**, 177 (1995).
17. E. Wiessenberger, P. Geltenbort, A. Oed, F. Gonnenwein, H. Faust, Nucl. Instrum. Methods A **248**, 506 (1986).
18. D. Hilscher, H. Rossner, Ann. Phys. (Paris) **17**, 471 (1992).
19. E. Holub, D. Hilscher, G. Ingold, U. Jahnke, H. Orf, H. Rossner, Phys. Rev. C **28**, 252 (1983).
20. V.E. Viola, K. Kwiatkowski, M. Walker, Phys. Rev. C **31**, 1550 (1985).
21. M.G. Itkis, L. Calabretta, F. Hanappe, Yu. M. Itkis, A. Kelic, N.A. Kondratiev, E.M. Kozulin, Yu. Ts. Oganessian, I.V. Pokrovsky, E.V. Prokhorova, G. Rudolf, A. Ya. Rusanov, L. Stuttge, Nucl. Phys. A **654** 870c (1999).
22. M. Strecker, R. Wien, P. Plischke, W. Scobel, Phys. Rev. C **41**, 2172 (1990).
23. C.J. Bishop, R. Vandenbosch, R. Aley, R.W. Shaw, I. Halpern, Nucl. Phys. A **150**, 129 (1970).